Molecular biomarker record of sea surface temperature and climatic change in the South China Sea during the last 140,000 years

Carles Pelejero [a,*], Joan O. Grimalt [a], Michael Sarnthein [b], Luejiang Wang [b], José-Abel Flores [c]

[a] *Department of Environmental Chemistry, CID-CSIC, Jordi Girona 18-26, 08034 Barcelona, Spain*
[b] *Institute of Geosciences, University of Kiel, D-24118 Kiel, Germany*
[c] *Department of Geology, Faculty of Sciences, University of Salamanca, 37008 Salamanca, Spain*

Abstract

The $\delta^{18}O$ and $\delta^{18}C$ isotopic composition of *Globigerinoides ruber,* the concentration of C_{37} alkenones, *n*-nonacosane and *n*-hexacosan-1-ol and the populations of coccolith species in core 17961-2 have been used to characterize the climatic changes which occurred in the South China Sea (SCS) during the last climatic cycle. The relative composition of di- and triunsaturated C_{37} alkenones, the U^K_{37} index, has been used to estimate the variation in sea surface temperatures. The concentrations of the terrigenous markers *n*-nonacosane and *n*-hexacosan-1-ol have allowed to infer changes in continental water dynamics during the glacial and interglacial times. The stratigraphic record of these compounds has shown that the influence of continental waters (i.e., the Molengraaff River) and restricted water circulation in SCS gave rise to a marginal system of higher but slower response to climatic change. Both in terminations I and II, the change from glacial to interglacial conditions involves a considerable reduction of continental water input into this semi-enclosed system. The high resolution study of the biomarker proxies in Termination I has shown that the SST increase lagged about 2.3 ky the $\delta^{18}O$ isotopic decrease of *Cibicidoides wuellerstorfi*. Probably, the SST increase corresponds to the period of the Sunda Shelf inundation onset. © 1999 Elsevier Science B.V. All rights reserved.

1. Introduction

The South China Sea (SCS) is a semi-enclosed system whose climate and hydrography has been significantly affected by the sea level changes. During glacial times, the Sunda Shelf was laid bare by the lower sea level and the rivers flowing from Southeast Asia, Malaysia, Sumatra and Borneo became very relevant for SCS hydrodynamics (Broecker et al., 1988). In this respect, the discharges of the Molengraaff or Paleo-Sunda River were of great importance. This river existed when the sea level was low and entered the South China Sea north of Western Borneo.

The paleoclimatic studies of these marginal seas require a good knowledge on the influence of the continental water dynamics during the glacial and interglacial periods. Thus, in addition to the study of climatic proxies such as sea surface temperature

* Corresponding author. Fax: +34 92 2045904;
E-mail: cpbqam@cid.csic.es

(SST) and isotopic records, comparison of the autochthonous and terrigenous inputs provide a useful tool for the understanding of hydrographic–climatic interactions.

To this end, useful information is contained in the sedimentary lipid composition. A portion of these compounds, the biomarkers, can be related with specific precursors and can be used as source of information on depositional input flux changes. Thus, *n*-nonacosane and *n*-hexacosan-l-ol are indicators of higher plant inputs (Eglinton and Hamilton, 1967). These compounds have been widely used as indicators of terrestrially derived higher plant inputs to the marine environment (Prahl and Pinto, 1987; Madureira et al., 1995; Schubert and Stein, 1996).

On the other hand, the C_{37} di-, tri- and tetra unsaturated alkenones are related with SST (Brassell et al., 1986a,b). These compounds can also be used as indicators of productivity of Haptophyceae, since they are specifically biosynthesized by these algae (Volkman et al., 1980; Marlowe et al., 1984). The relationship between C_{37} alkenones composition and water temperature is based on the degree of unsaturation of the ketone distributions which is measured by means of several indices:

$$U_{37}^K = (C_{37:2} - C_{37:4})/(C_{37:2} + C_{37:3} + C_{37:4})$$

$$U_{37}^{K'} = C_{37:2}/(C_{37:2} + C_{37:3})$$

where $C_{37:4}$, $C_{37:3}$ and $C_{37:2}$ are the concentrations of heptatriaconta-(8E, 15E, 22E, 29E)-tetraen-2-one, heptatriaconta-(8E, 15E, 22E)-trien-2-one and heptatriaconta-(15E, 22E)-dien-2-one, respectively.

Both indices are equal when $C_{37:4} \to 0$. U_{37}^K determinations in isothermally cultured *Emiliania huxleyi*, the most abundant coccolithophorid species in the present oceans (Marlowe et al., 1984), showed that the relationship was linear in a range of 8 to 25ºC (Prahl and Wakeham, 1987, Prahl et al., 1988).

In a recent work, the relationship between U_{37}^K and the SST has been calibrated for the SCS (Pelejero and Grimalt, 1997). A good linearity has been found, showing that the U_{37}^K index can also be used for paleotemperature reconstructions in the warm waters (25–29ºC) of this marginal sea. The equation encountered, $U_{37}^K = 0.031T + 0.092$, is very similar to the equation published for *E. huxleyi* cultures and column water samples ($U_{37}^K = 0.033T + 0.043$; Prahl and Wakeham, 1987), which has often been used in paleoclimatic work. The correlation between U_{37}^K and temperatures in the SCS is valid for the annually averaged water mass between 0 and 30 m.

The present work is focussed on the study of the molecular biomarker data in core 17961-2, obtained from the Sunda Slope (Fig. 1). High resolution profiles of C_{37} and C_{38} *alkenones,* U_{37}^K-SST, *n*-nonacosane and *n*-hexacosan-1-ol have been determined in Barcelona. These profiles have been interpreted by reference to the $\delta^{18}O$ and $\delta^{13}C$ isotopic composition of *Globigerinoides ruber* performed in Kiel. The composition of coccolith species and their sedimentary abundances have been determined in Salamanca for further assessment of the depositional environments and significance of the alkenone data. A selected time horizon summary of these parameters is shown in Table 1.

2. Materials and methods

The sediment samples considered in this study were obtained from gravity core 17961-2 (8º30.4′N, 112º19.9′E, 1968 m depth), collected in the Sunda Slope (Fig. 1) during the R/V *Sonne* 95 cruise (April–June 1994; Sarnthein et al., 1994). Sediment sections were subsampled at spacings of 4–10 cm in 1 cm intervals over the total core length, 992 cm.

The core sections have been dated by comparison of the $\delta^{18}O$ isotopic record of *G. ruber* and *Cibicidoides wuellerstorfi* with the SPECMAP normalized isotope curve (Martinson et al., 1987) and 4 accelerator mass spectrometry (AMS) ^{14}C datings, which have been converted to calendar ages according to Bard et al. (1990) as summarized in Table 2. Planktonic biostratigraphy is coincident with the age model. This shows the *E. huxleyi* Acme (about 85 kyr) at 845 cm and the last appearance of the pink-pigmented variant of *G. ruber* (Stage 5e) at 960 cm. The *G. ruber* $\delta^{18}O$ profile versus depth and calendar ages is represented in Fig. 2, where the AMS ^{14}C dates and the biostratigraphic references used for calibration are also indicated (for $\delta^{18}O$ data on *C. wuellerstorfi*, see L. Wang et al., 1999). The core bottom has been reported to be compacted with the consequent reduction of the observed sedimentation rate.
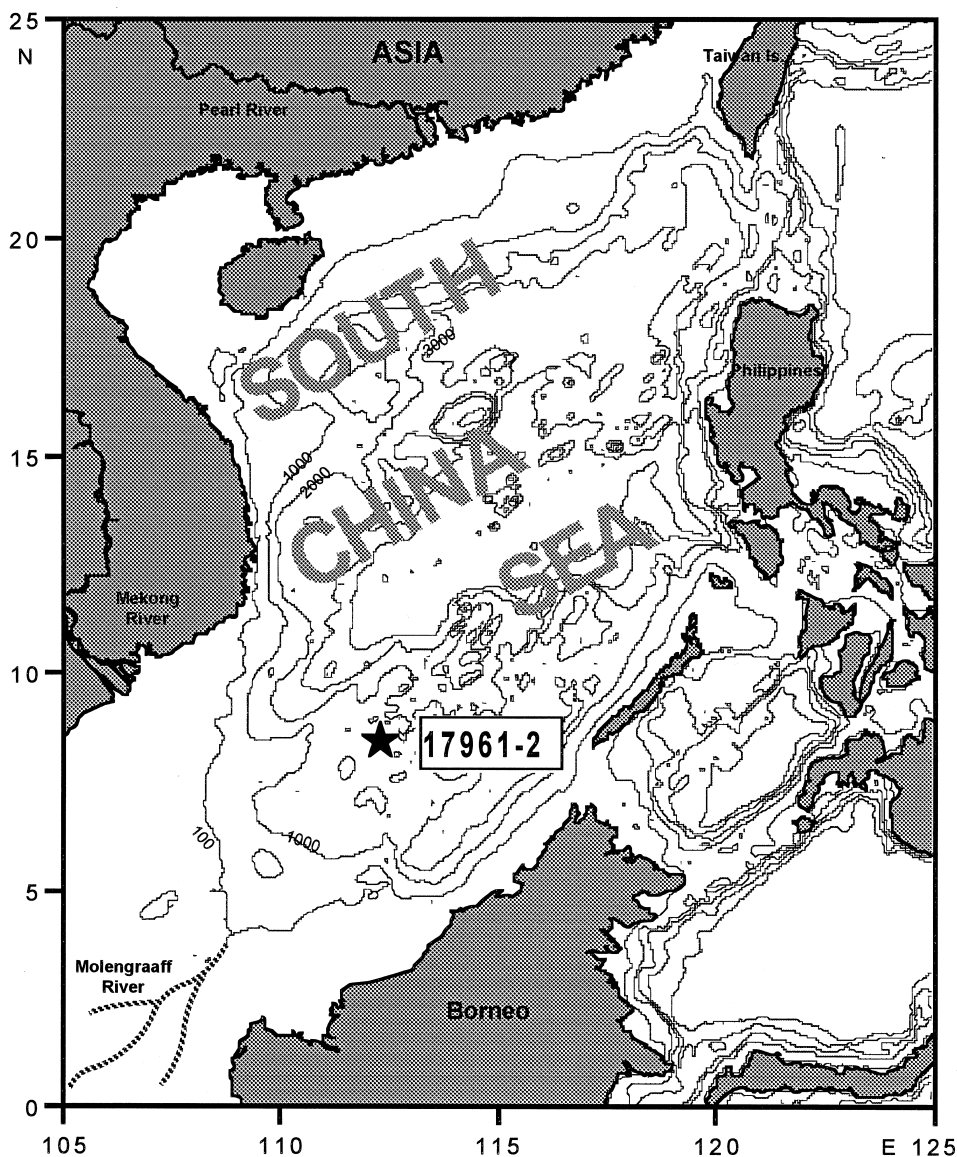
Fig. 1. Map of the South China Sea showing the location of core 17961-2. The estimated Molengraaff river track during glacial times is indicated. (Note that the 100 m isobath approximately represents the coastline during glacial times).

The procedures and equipment used for the U_{37}^K index determinations are described elsewhere (Villanueva et al., 1997). Briefly, sediment samples were freeze-dried and manually ground for homogeneity. After addition of an internal standard of *n*-hexatriacontane, approximately 3 g of dry sediment were extracted in an ultrasonic bath with dichloromethane and the extracts were hydrolyzed with 6% potassium hydroxide in methanol to eliminate wax ester interferences. After derivatizing with bis(trimethyisilyl)trifluoroacetamide, the extracts were analyzed by gas chromatography with flame ionization detection. Selected samples were examined by gas chromatography coupled to mass spectrometry to confirm compound identification and check for possible coelutions.

Table 1
Summary of parameter values for selected time horizons

	Modern times	LGM	Stage 3 average	Stage 5e	Stage 6
$\delta^{18}O$ *G. ruber* ‰ PDB	−3.12	−1.72	−2.39	−3.19	−1.89
SST (ºC)	28	25.2	26	29.2	26.5
Nonacosane (ng/g)	27	150	133	25	155
Hexacosan-1-ol (ng/g)	90	280	234	75	245
$\delta^{13}C$ *G. ruber* ‰ PDB	1.63	1.32	1.29	0.78	0.86
F. profunda (coccolith/g)	19.2×10^9	6.0×10^9	6.4×10^9	23.0×10^9	5.5×10^9
C_{37} alkenones (ng/g)	511	600	800	570	1060
E.hux/G.oce	3.1	1.2	1.5	1.19	0.21
K_{37}/K_{38}	1.20	1.16	1.20	1.34	1.15
%CaC0$_3$	35	13	10	27	12

SST data obtained using the equation of Pelejero and Grimalt (1997), which represents annual average temperatures between 0 and 30 m depth. E.hux/G.oce refers to the ratio between *E. huxleyi* and *G. oceanica* coccoliths. K_{37}/K_{38} indicates to the ratio between C_{37} and C_{38} alkenones.

The slides used to inventory the coccolithophore assemblages were prepared using the methodology of Flores et al. (1995), which affords homogeneous and comparable data among different samples. Measurement of sediment weight, spreading and observation surfaces allowed the estimation of surface coccolith density (coccoliths per mm^2) and subsequent conversion to sedimentary coccolith abundances.

3. Results and discussion

3.1. SST evolution over the last climatic cycle

A representative chromatogram of the neutral lipid composition of SCS sediments is shown in Fig. 3. Since no $C_{37:4}$ has been found in any of the sediment sections, the previously mentioned U_{37}^K and $U_{37}^{K'}$ are identical. The conversion of U_{37}^K into SST has been performed with the above mentioned

equation specifically calibrated for the SCS using the annual average SST at 0–30 m depth (Pelejero and Grimalt, 1997). The resulting SST profile is shown in Fig. 4. The SST estimates for the undisturbed sediment surfaces (0–1 cm depth) obtained with this equation matched exactly the modern annual 0–30 m depth average SST for this region (28.0ºC, Levitus, 1994).

For comparison, the SST results derived from the U_{37}^K equation calibrated by Prahl and Wakeham (1987) from *E. huxleyi* cultures are also represented in Fig. 4. The variation among the two curves is smaller than 0.2ºC and differences can only be observed at the warmer temperatures. The sole observation of discrepancies at warm temperatures was a priori expected because the calibration equation based on *E. huxleyi* cultures did not include points in the high temperature range. Conversely, the SCS equation was addressed to temperature calibration at this warm range. Based on five replicate

Table 2
AMS ^{14}C ages dated in core 17961-2 (L. Wang et al., 1999)

Sample depth (cm)	AMS ^{14}C age (yr BP)	Corrected AMS ^{14}C age (yr BP)	Error 1 − sigma ±(yr)	Calibrated age (yr BP)
290	24,940	24,540	+290/−280	28,040
310	25,880	25,480	+340/−330	28,980
440	34,600	34,200	+940/−840	37,700
490	40,100	39,700	+2100/−1700	43,200

Under 'Corrected AMS ^{14}C age', a 400-yr correction has been applied for the reservoir age of sea water, although its precise age range is unknown in the South China Sea (Stuiver and Braziunas, 1993). Conversion from ^{14}C kyr BP to calibrated kyr BP after Bard et al., 1990. All datings were performed on single species (*Globigerinoides sacculifer*).
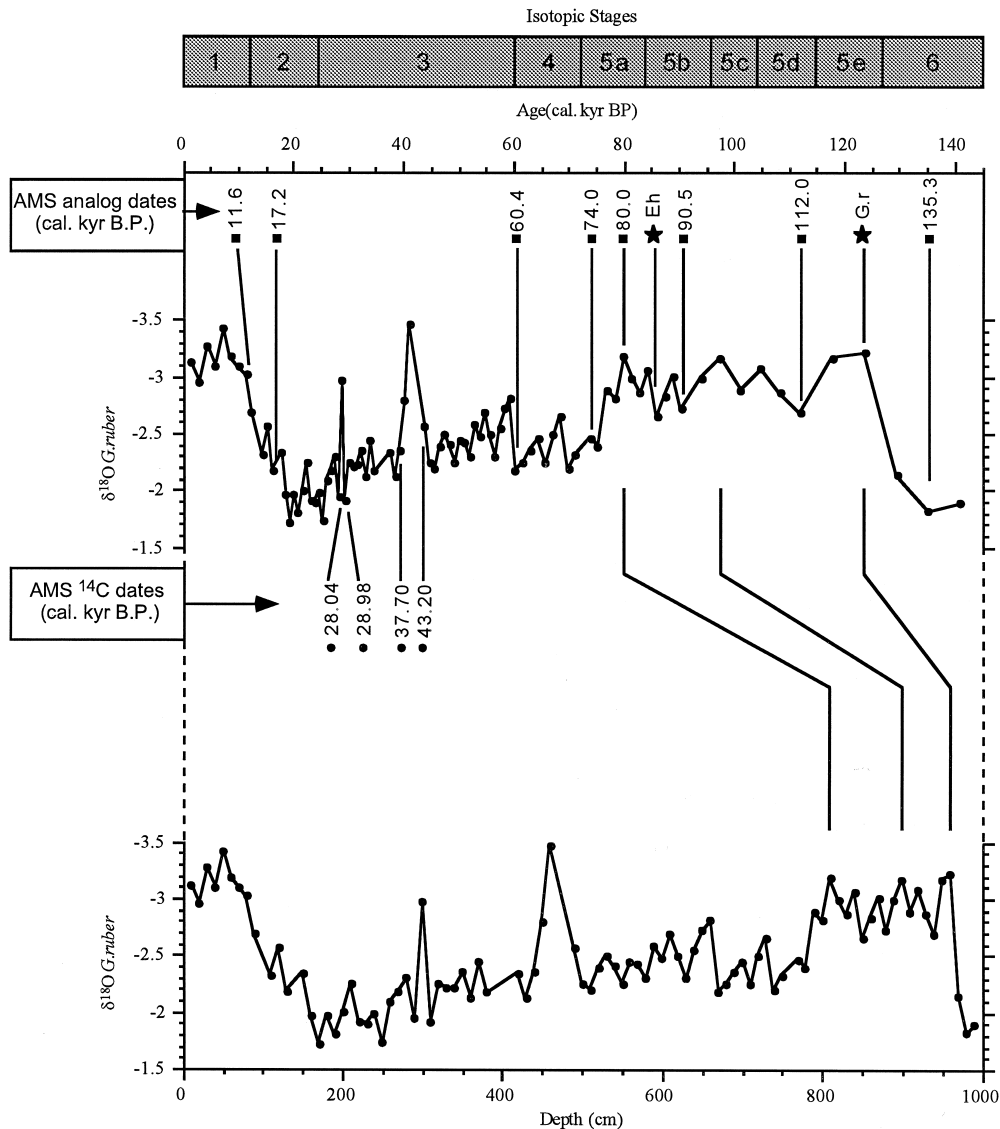
Fig. 2. Time scale of core 17961-2 based on the δ^{18}O isotopic composition of *G. ruber* and *C. wuellerstorfi* (not depicted, see L. Wang et al., 1999), AMS ^{14}C dating and planktonic biostratigraphy. Filled squares show ages of AMS analog oxygen isotope chronostratigraphy (the first three ages from the top based on Winn et al. (1991) and the rest based on Martinson et al. (1987). Eh represents the timing of *E. huxleyi* Acme and G.r relates to the last appearance of the pink-pigmented variant of *G. ruber*. Filled circles show the calibrated ages of the 4 AMS datings performed in the core (see Table 1).

analyses of deep sea sediments containing similar alkenone abundances, the analytical error involved in the U^{K}_{37}-SST measurement is of ±0.15°C.

The SST of core 17961-2 range within 25–29°C (Fig. 4). In general, the SST profile follows the *G. ruber* δ^{18}O isotopic curve (Fig. 4), exhibiting a typical glacial to interglacial pattern. The difference

between modern times and the Last Glacial Maximum (LGM) is 2.8°C. Differences of 1.3°C, 1.8°C and up to 1.5°C have been reported for SST reconstructions based on the U^{K}_{37} index in the eastern Equatorial Pacific (Prahl et al., 1989), the central Equatorial Atlantic (Sikes and Keigwin, 1994) and the western Tropical Pacific (Ohkouchi et al., 1994),
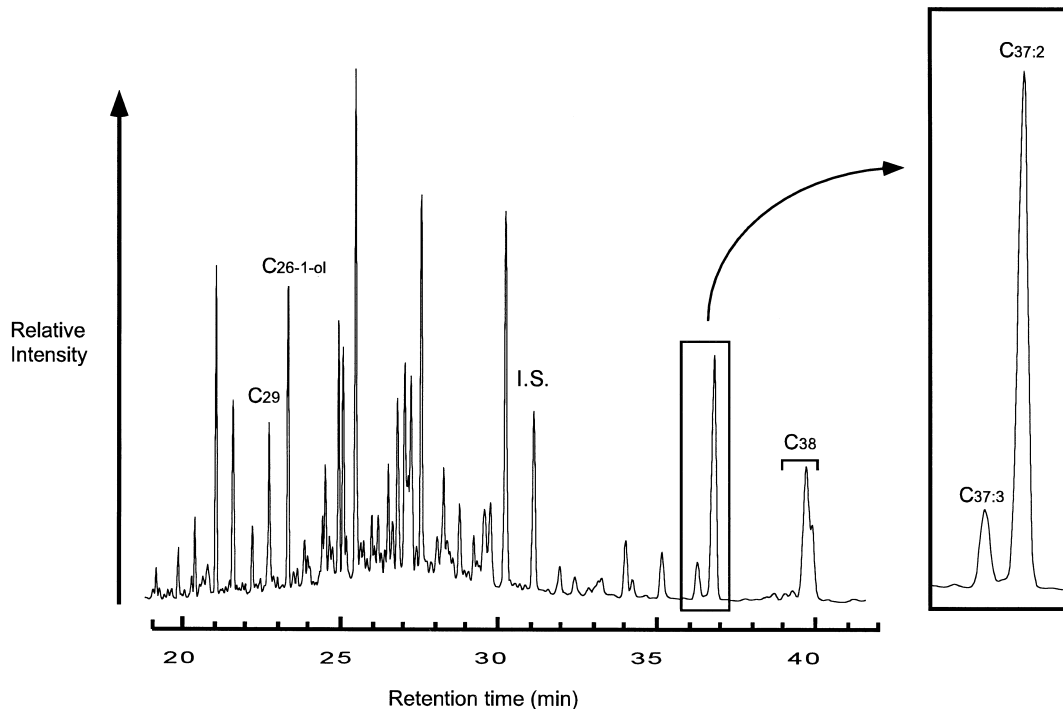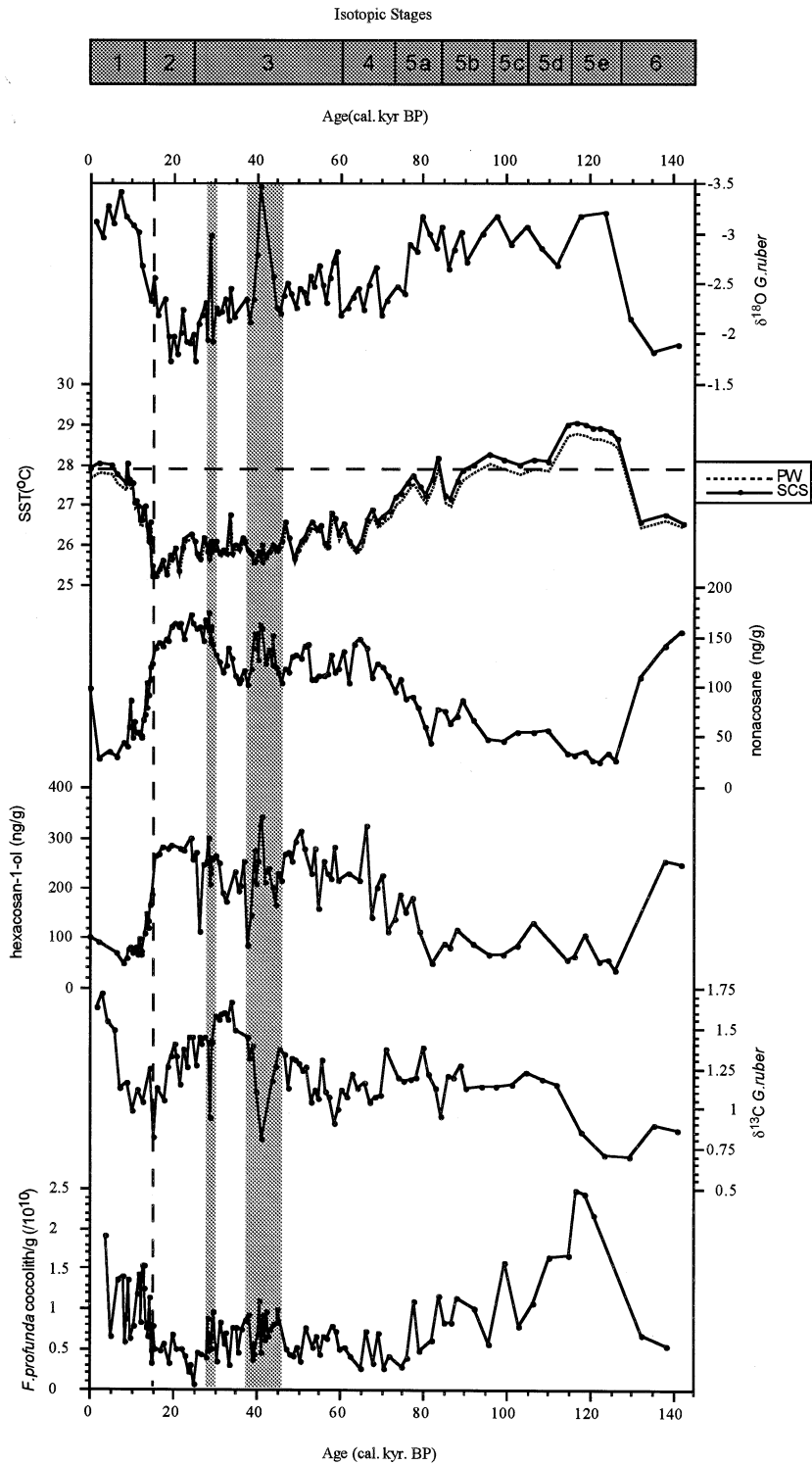
Fig. 3. Representative gas chromatogram of the neutral lipid composition of the South China Sea sediments. The peaks corresponding to *n*-nonacosane (C$_{29}$), *n*-hexacosan-1-ol (C$_{26\text{-}1\text{-}ol}$), heptatriaconta-(8E,15E,22E)-trien-2-one (C$_{37:3}$) and heptatria-conta-(15E,22E)-dien-2-one (C$_{37:2}$) are indicated. I.S.: internal standard (*n*-hexatriacontane). The region of appearance of C$_{38}$ alkenones is marked as C$_{38}$.

respectively. Likewise, the results obtained in the extensive work of the CLIMAP project (CLIMAP Project Members, 1981) based on planktonic microfossils also show variations lower than 2°C between LGM and present times in low latitude open oceans. In this respect, the glacial–interglacial δ^{18}O amplitude in the SCS record, 1.7‰, is also higher than in equivalent latitude open oceans and in close seas like the Sulu Sea, 1.3‰ (Linsley, 1996).

The temperature differences in the continental areas of the same latitudes are of higher magnitude than those observed in the SCS. This is indicated by the 1 km lowering of the snowline (Broecker

and Denton, 1989 and references therein) and vegetation changes (Sun and Li, 1999). Furthermore, foraminiferal assemblage SST measurements in the SCS have evidenced an enhanced seasonality, with considerably colder winters, in the glacial times (L. Wang and P. Wang, 1992; Pflaumann et al., 1999; P. Wang, 1999). Then, the temperature difference of Transition I (Fig. 4) shows that the SCS has been more sensitive to climate change than the open ocean regions. Possibly its restricted water circulation led to greater difficulties of heat exchange and temperature homogenization in glacial than interglacial times. Thus, in glacial times the influence of the land

Fig. 4. δ^{18}O and δ^{13}C isotopic composition of *G. ruber*, U$^{K}_{37}$ sea surface temperature (SST), *n*-nonacosane, *n*-hexacosan-1-ol and *F. profunda* sedimentary abundances in core 17961-2 during the last 140 kyr. *PW* (dotted line) and *SCS* (solid line) show the SST records calculated with the equations of Prahl and Wakeham (1987) and Pelejero and Grimalt (1997), respectively. The latter equation represents annual average temperatures for 0–30 m depth. Vertical dashed line marks the timing (14.9 kyr B.P.) of the abrupt increase in SST and decrease in terrestrial marker concentrations which is probably coincident with the onset of the inundation of the Sunda Shelf. Horizontal dashed line marks the SST for modern times. Note the higher SST temperatures (1.2 degree approx.) during Stage 5e in relation to Stage 1. Shaded areas indicate the timing of the extremely high precipitation events recorded in the isotopic curves (see text).

masses may have been important in this marginal sea, particularly for the enhanced river hydrodynamics. Recently, two studies based on U_{37}^K reconstructions in the SCS have revealed an even higher temperature difference between LGM and modern times (3.5–4ºC), for two cores located further north (17–18ºN; Huang et al., 1997a,b).

In this respect, the close examination of Termination I shows that the 3ºC SST increase lags the *G. ruber* $\delta^{18}O$ isotope decrease by about 4.5 kyr but is coincident with a decrease in $\delta^{13}C$ isotopic content of *G. ruber* (Fig. 4). This isotopic decrease occurs at about 19.5 kyr B.P., so more than 2 kyr earlier than the onset of Termination I at 17.2 kyr B.P., (see the *C. wuellerstorfi* $\delta^{18}O$ curve for the same station; L. Wang et al., 1999), and may be ascribed to a period of extreme precipitation and river runoff involving a low in salinity (L. Wang et al., 1999). The age of the SST increase, 14.9 kyr B.P., probably corresponds to the beginning of the inundation of the Sunda Shelf. Although the exact timing of the complete inundation is still not well constrained, Broecker et al., 1988 suggested that it occurred slightly after 13 kyr B.P. Likewise, the abrupt SST increase may have resulted from the discontinuation of the influence of the cold waters from the Molengraaff and other main rivers into the SCS, as well as from the lateral advection of warm water through the Borneo strait (P. Wang, 1999). In these conditions, the massive input of seawater may have led to an episode of higher productivity as recorded in the $\delta^{13}C$ isotope record.

During isotopic Stage 5 (127–72 kyr BP), the $\delta^{18}O$ curve exhibits the changes characteristic of the five substages 5a to 5e, with very similar isotope values in the warm substages 5a, 5c and 5e (−3.2‰). Differently, the SST of Stage 5e (127–116 kyr BP), 29.2ºC, is considerably warmer than that found in the other warm substages (28–28.2ºC). It is also worth to note the stability of the warm conditions within the Stage 5e. Roughly millennial-resolution during the 11 kyr of this sub-stage show that SST increased smoothly from 28.7ºC to 29.2ºC and then fell to 28ºC in Stage 5d (Fig. 4).

Comparison of Stage 5e and Holocene temperatures shows that the former was 1.2ºC warmer than present times. These results are in agreement with foraminiferal countings in another SCS core, V36-06-3, which led to conclude that winter temperatures

in Stage 5e were about 2ºC warmer than in the Holocene (L. Wang and P. Wang, 1992). Thus, the generally accepted scenario of similar SST for the last two interglacial periods (CLIMAP Project Members, 1984) is not applicable to this marginal sea. In fact, comparison of populations of gastropods in other marginal seas such as the Mediterranean also revealed a warmer climate in Stage 5e than in the Holocene (Cornu et al., 1993). Evidence of a warmer Stage 5e has also been observed in open ocean areas, like in the mid-latitude North Atlantic, where U_{37}^K-SST reconstruction shows a temperature difference of 3ºC between these two interglacial periods (Villanueva, 1996; Madureira et al., 1997). A warmer Stage 5e was also recorded from biotic census counts in several cores from the North Atlantic (CLIMAP Project Members, 1984). The recurrent evidences of eustatic sea levels roughly 6 m higher for the last interglacial than today, and many other land and oceanic evidences (CLIMAP Project Members, 1984 and references therein), suggest that a warmer interglacial could be recorded in many more sites than previously thought. Even in the Antarctica, the δD record of the last interglacial air temperatures indicate 2ºC warmer conditions than present (Jouzel et al., 1987).

The SST data of Fig. 4 also display a SST difference between Stages 2 and 6 showing that the LGM was 1.4ºC cooler than Stage 6. This difference is in agreement with the winter temperature variations found in core V36-06-3 with foraminiferal population studies (L. Wang and P. Wang, 1992). The same SST trend between the two stages has been observed from U_{37}^K-SST reconstructions in the North Atlantic (Villanueva, 1996).

3.2. Short isotopic events

The isotopic $\delta^{18}O$ profile in Stage 3 (24–60 kyr) show two prominent peaks at 290–310 and 430–500 cm, which have been AMS ^{14}C dated precisely to 28.0–29.0 and 37.7–~43.2 calendar kyr B.P., respectively (Fig. 4, Table 2). The lack of specific SST signal in relation to these two isotopic events leads to infer two episodes of low sea surface salinity (SSS) caused by extreme tropical precipitation and enhanced summer monsoon activity. These episodes were also characterized by considerably
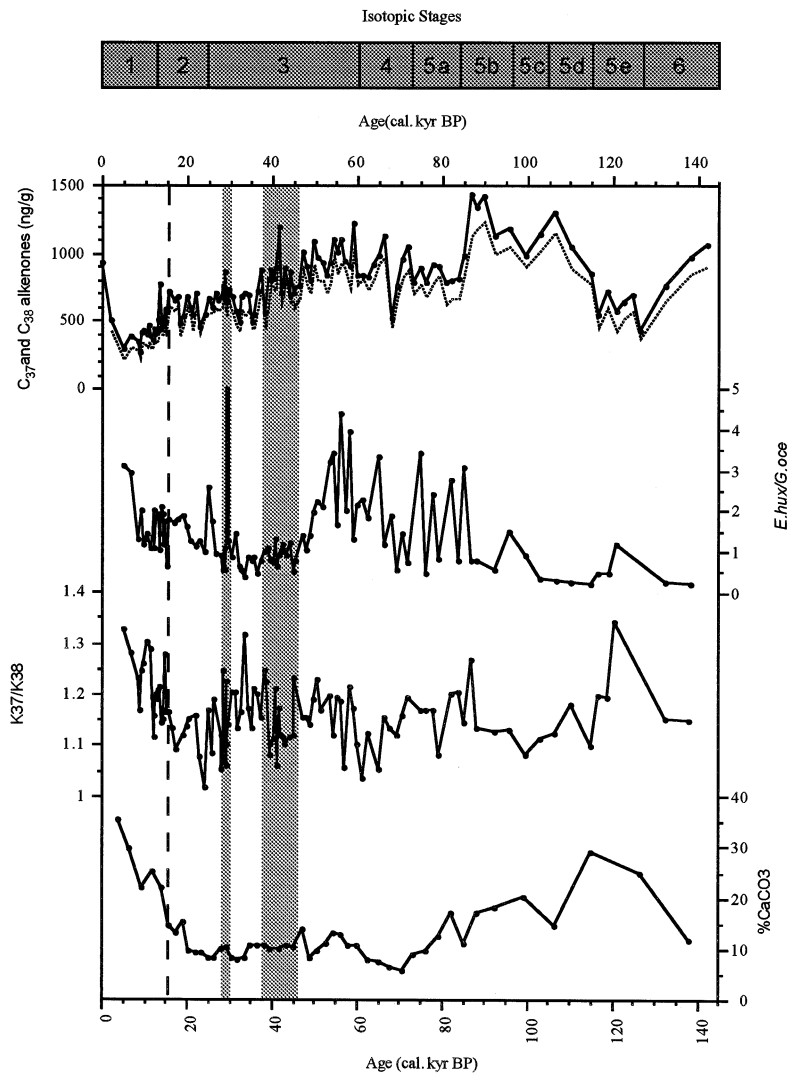
Fig. 5. Concentrations of C_{37} (solid line) and C_{38} alkenones (dotted line) in ng/g dry sediment, *E. huxleyi/G. oceanica* coccolith abundance ratio, C_{37}/C_{38} alkenone ratio and calcium carbonate content in core 17961-2 during the last 140 kyr. The C_{37}/C_{38} alkenone ratio is only displayed using the samples for which coccolith data was available. Vertical dashed line and shaded areas as in Fig. 4.

fertility increases as evidenced by the strong $\delta^{13}C$ isotope decreases at these events (Fig. 4). This increase in productivity is also detected in the long chain alkenone record (Fig. 5; note that the alkenone record has a higher time resolution).

Interestingly, these two low salinity events occurred very close in time to Heinrich events 3 and 4 in the North Atlantic. Porter and Zhisheng (1995) in their study of Chinese loess grain-size data observed enhanced eolian dust transport and deposition

events in coincidence with most of the Heinrich layers recorded in the North Atlantic. Increased strength of East Asian winter monsoon during the time of Heinrich events in the North Atlantic was inferred from their measurements. In their study, Heinrich layers 3 and 4 were occurring at 27 ^{14}C kyr (~31 cal kyr BP) and 35 ^{14}C kyr (~39.5 cal kyr BP), respectively. Comparing with these datings, the older abrupt low salinity event of core 17961-2 could be coincident with Heinrich event 4 but the younger

would have occurred about 2 kyr later. There is, however, some uncertainty concerning the dates of these salinity events due to the lack of information on ^{14}C production rate, especially during isotope Stage 3. Furthermore, the dates of the Heinrich events are also under discussion. Thus, Bond et al. (1993) dated Heinrich event 4 at 35.5 ^{14}C kyr ($\sim$40 cal kyr BP) while Manighetti et al. (1995) estimated an age of 39 14 C kyr (43 cal kyr BP). As L. Wang et al. (1999) suggested, these low salinity events could also be ascribed to warm Dansgaard-Oeschger events 8 and 4/3 (Grootes and Stuiver, 1997), respectively.

3.3. Terrigenous organic matter inputs

The concentrations of n-nonacosane and n-hexacosan-1-ol in core 17961-2 are shown in Fig. 4. In general both compounds exhibit a parallel trend which is in agreement with their common higher plant origin. These profiles evidence that the period of highest flux of terrigenous materials was between 30 and 15 kyr B.P.

The main trend of these two compounds is an inverse correlation with SST throughout all core. The lowest n-nonacosane concentrations (20 ng/g) are found at high temperatures (Stages 1 and 5) and the highest concentrations (160–170 ng/g) at low temperatures (Stages 2–4).

The inverse correlation between these terrigenous markers and SST is in agreement with erosional changes of the continental platform as consequence of the glacial/interglacial sea level oscillations. As has been mentioned in Section 1, as consequence of the general sea level decrease during glacial times, a huge river flow appeared north of Western Borneo, the so called Molengraaff or Paleo-Sunda River. The approximate track of this river flow during glacial times (sea level decrease of about 100 m) has been plotted in Fig. 1. Thus, terrigenous markers in the location of core 17961-2 are likely reflecting the flow changes of the material transported by this river which, in turn, might have been influenced by sea level and precipitation changes.

In this respect, the SST rise corresponding to Termination I is coincident with an abrupt decrease of terrigenous markers (Fig. 4). The onset of the inundation of the Sunda Shelf (Broecker et al., 1988) might have resulted in the deposition of the terrigenous sediments closer to the present coastline and therefore further away from the core location. Similar changes in SST, n-nonacosane and n-hexacosan-1-ol concentrations are also observed at the end of Stage 6 (Fig. 4).

In addition to the general glacial/interglacial trend, some specific features related with the changes in concentration of n-nonacosane and n-hexacosan-1-ol have to be considered. Thus, the above described two low salinity events recorded in the δ^{18}O $G.$ $ruber$ curve are coincident with higher values of the terrestrial markers. This increase in n-nonacosane and n-hexacosan-1-ol describes higher contributions of terrigenous organic matter as consequence of the higher precipitation which led to these two low salinity events.

3.4. The coccolith contribution and long chain alkenones record

The carbonate content follows a glacial/interglacial pattern, with higher abundances in the interglacials (Fig. 5). The low concentrations during glacial periods may be a consequence of dilution by terrestrial matter (Schönfeld and Kudrass, 1993). A remarkable feature of the coccolith composition consists of the high abundances of $F.$ $profunda$ throughout all core, with values ranging from 50 to 90% of the total coccolith (Fig. 4). The alkenone producers, $E.$ $huxleyi$ and $Gephyrocapsa$ $oceanica$ are also found but at lower percentages, with minimum values during Stage 5. In this stage, the second major coccolith besides $F.$ $profunda$ is constituted by very small $gephyrocapsa$.

An abrupt five-fold increase in the abundance of $F.$ $profunda$ is observed at 14.9 kyr B.P. (Fig. 4) which parallels the SST increase at this time. The increase of this species may mark a rapid change from a shallow to a deep nutricline, leading to more stratified and less productive waters after the SST increase (Okada and Honjo, 1973; Molfino and Mcintyre, 1990). The alkenone production capability of $F.$ $profunda$ is unknown (Brand, 1994). However, the important increase of this species in Stage 1 is followed by a decrease of alkenone concentration (Figs. 4 and 5) which could suggest that these algae do not synthesize long chain alkenones, and would support the decrease in productivity associated with

stratification. A similar trend is observed in Stage 5e where the high abundance of *F. profunda* occurs simultaneously to a decrease in C_{37} and C_{38} alkenones.

In relation to the coccolith species present in lower abundance than *F. profunda*, the relative composition of *E. huxleyi* and *G. oceanica* can be monitored by the ratio of C_{37} to C_{38} alkenones (Volkman et al., 1995). As shown in Fig. 5, the concentrations of C_{37} and C_{38} alkenones exhibit a rather parallel trend and the C_{37}/C_{38} ratios range between 1–1.4. These values are in principle more similar to those encountered in *E. huxleyi* cultures (Prahl et al., 1988). The values for *G. oceanica* reported in the literature are below 1 (Volkman et al., 1995) and are not encountered in core 17961-2 which likely reflects a low contribution of *G. oceanica* to the total C_{37} alkenone content of this core.

The elucidation of the relative abundance of *E. huxleyi* vs. *G. oceanica* is significant for the differences in U^K_{37}-SST calibration curves reported for these two Haptophyceae (Prahl and Wakeham, 1987; Volkman et al., 1995). However, the two reported straight lines converge at the warm end and provide similar temperature values in the 25–29ºC range. Thus, no significant SST changes are expected from variations of relative composition of *E. huxleyi* and *G. oceanica* in the SCS cores.

The alkenone abundance profile (Fig. 5.) shows the highest amounts during Stage 5, reaching concentration values of about 1.4 µg/g dry sediment for the C_{37} species. After this stage, the alkenones decrease progressively till the modern day value of 0.5 µg/g dry sediment. The comparison of these alkenone results with *F. profunda* abundances shows an inverse correlation (Figs. 4 and 5), which again is consistent with lower abundance of alkenone-producing Haptophyceae species in more stratified and less productive waters.

4. Conclusions

In the SCS the influence of continental waters (i.e., the Molengraaff River) and restricted water circulation gave rise to a marginal system of higher but slower sensitivity to climatic change. Thus, in Termination I the SST difference between the LGM

and Holocene is 2.8ºC whereas only 1.3–1.8ºC SST increases are observed in open ocean areas of the same latitude. However, this temperature increase lagged about 2 kyr the $\delta^{18}O$ isotopic decrease of *C. wuellerstorfi*. The SST change was probably coincident with the onset of the inundation of the Sunda Shelf, a considerable decrease of continental water input and concurrent with the development of a deep nutriocline. These effects can be recognized in the concentration changes of *n*-nonacosane and *n*-hexacosan-1-ol and the sedimentary abundances of *F. profunda*, respectively. The concentrations of terrigenous markers are eight times lower in the Holocene than before the LGM.

Similar increases in SST and decreases in *n*-nonacosane and *n*-hexacosan-1-ol are observed at the transition between Stages 6 and 5e (Termination II). These parallel changes in both terminations suggest that the development of interglacial conditions involved the same modifications in water hydrodynamics as those occurred in Termination I particularly a considerable reduction of continental water input. In this respect, the SST of the SCS waters in Stage 5e was 1.2ºC warmer than the Holocene, a feature that has also been observed in many other ocean regions. These warm conditions were maintained during the 11 ky of this sub-stage.

Two marked episodes of extreme water precipitation and productivity increase have been observed during Stage 3. These episodes are reflected in the $\delta^{18}O$ and $\delta^{13}C$ isotopic composition, SST and *n*-nonacosane and *n*-hexacosan-1-ol concentrations. Careful AMS ^{14}C datings have shown that one of these episodes is coincident in time with Heinrich layer 4 in the North Atlantic and the other occurred about 2 kyr later than H3. However, further dating information is needed to confirm or disregard a teleconnection between these two types of climatic events.

stages of this work. We are grateful to G. Eglinton and A. Rosell-Meld for detailed and constructive reviews.

References

Bard, E., Hamelin, B., Fairbanks, R.C., 1990. U–Th ages obtained by mass spectrometry in corals from Barbados: sea level during the past 130,000 years. Nature 346, 456–458.

Bond, G., Broecker, K., Johnsen, S., McManus, J., Labeyrie, L., Jouzel, J., Bonani, G., 1993. Correlations between climatic records from North Atlantic records from North Atlantic sediments and Greenland ice. Nature 365, 143–147.

Brand, L.E., 1994. Physiological ecology of marine coccolithophores. In: Winter, A., Siesser, W.G. (Eds.), Coccolithophores. Cambridge University Press, 42 pp.

Brassell, S.C., Eglinton, G., Marlowe, I.T., Pflaumann, U., Sarnthein, M., 1986a. Molecular stratigraphy: a new tool for climatic assessment. Nature 320, 129–133.

Brassell, S.C., Brereton, R.G., Eglinton, G., Grimalt, J., Liebezeit, G., Marlowe, I.T., Pflaumann, U., Sarnthein, M., 1986b. Palaeoclimatic signals recognized by chemometric treatment of molecular stratigraphic data. Org. Geochem. 10, 649–660.

Broecker, W.S., Denton, G.H., 1989. The role of ocean–atmosphere reorganizations in glacial cycles. Geochim. Cosmochim. Acta 53, 2465–2501.

Broecker, W.S., Andree, M., Klas, M., Bonani, G., Wolfli, W., Oeschger, H., 1988. New evidence from the South China Sea for an abrupt termination of the last glacial period. Nature 333, 156–158.

CLIMAP Project Members, 1981. Seasonal reconstructions of the earth's surface at the last glacial maximum. Geol. Soc. Am. Map and Chart Series 36, 11–18.

CLIMAP Project Members, 1984. The Last Interglacial Ocean. Quat. Res. 21, 123–224.

Cornu, S., Pätzold, J., Bard, E., Meco, J., Cuerda-Barcelo, J., 1993. Paleotemperature of the last interglacial period based on $\delta^{18}O$ of Strombus bubonius from the western Mediterranean Sea. Palaeogeograph. Palaeoclimat. Palaeoecol. 103, 1–20.

Eglinton, G., Hamilton, R.J., 1967. Leaf epicuticular waxes. Science 156, 1322–1335.

Flores, J.A., Sierro, F.J., Raffi, I., 1995. Evolution of the Calcareous Nannofossil assemblage as response to the paleoceanographic changes in the Eastern Equatorial Pacific Ocean from 4 to 2 Ma (Leg 138, Sites 849 and 852). Proc. ODP Sci. Results 138, 163–176.

Grootes, P.M., Stuiver, M., 1997. Oxygen 18/16 variability in Greenland snow and ice with 10^{-3} to 10^{-5} year time resolution. J. Geophys. Res. 102, 26455–26470.

Huang, C.-Y., Wu, S.-F., Zhao, M., Chen, M.-T., Wang, C.-H., Tu, W., Yuan, P.B., 1997a. Surface ocean and monsoon climate variability in the South China Sea since the last glaciation. Mar. Micropaleontol. 32, 71–94.

Huang, C.-Y., Liew, P.-M., Zhao, M., Chang, T.-C., Kuo, C.-M.,

Chen, M.-T., Wang, C.-K., Zheng, L.-F., 1997b. Deep sea lake records of the Southeast Asian paleomonsoons for the last 25 thousand years. Earth Planet. Sci. Lett. 146, 59–72.

Jouzel, J., Lorius, C., Petit, J.R., Genthon, C., Barkov, N.I., Kotlyakov, V.M., Petrov, V.M., 1987. Vostok ice core: a continuous isotope temperature record over the last climatic cycle (160,000 years). Nature 329, 403–408.

Levitus, S., 1994. World Ocean Atlas. NOAA NESDIS, U.S. Govt. Printing Office.

Linsley, B.K., 1996. Oxygen-isotope record of sea level and climate variations in the Sulu Sea over the past 150,000 years. Nature 380, 234–237.

Madureira, L.A.S., Conte, M.H., Eglinton, G., 1995. Early diagenesis of lipid biomarker compounds in North Atlantic sediments. Paleoceanography 10, 627–642.

Madureira, L.A.S., van Kreveld, S.A., Eglinton, G., Conte, M.H., Ganssen, G., van Hinte, J.E., Ottens, J.J., 1997. Late Quaternary high-resolution biomarker and other sedimentary climate proxies in a northeast Atlantic core. Paleoceanography 12, 255–269.

Manighetti, B., McCave, I.N., Maslin, M., Shackleton, N.J., 1995. Chronology for climate change: Developing age models for the biogeochemical ocean flux study cores. Paleoceanography 10, 513–525.

Marlowe, I.T., Green, J.C., Neal, A.C., Brassell, S.C., Eglinton, G., Course, P.A., 1984. Long-chain alkenones in the Prymnesiophyceae. Distribution of alkenones and other lipids and their taxonomic significance. Br. Phycol. J. 19, 203–216.

Martinson, D.G., Pisias, N.G., Hays, J.D., Imbrie, J., Moore, T.C., Shackleton, N.J., 1987. Age dating and the orbital theory of the ice ages: Development of a high resolution 0–300,000-year chronostratigraphy. Quat. Res. 27, 1–29.

Molfino, B., Mcintyre, A., 1990. Precessional forcing of nutricline dynamics in the Equatorial Atlantic. Science 249, 766–769.

Ohkouchi, N., Kawamura, K., Nakamura, T., Taira, A., 1994. Small changes in the sea surface temperature during the last 20,000 years: Molecular evidence from the western tropical Pacific. Geophys. Res. Lett 21, 2207–2210.

Okada, H., Honjo, S., 1973. The distribution of oceanic coccolithophorids in the Pacific. Deep-Sea Res. 20, 355–374.

Pelejero, C., Grimalt, J.O., 1997. The correlation between the U_{37}^K index and sea surface temperatures in the warm boundary: The South China Sea. Geochim. Cosmochim. Acta 61, 4789–4797.

Porter, S.C., Zhisheng, A., 1995. Correlation between climate events in the North Atlantic and China during the last glaciation. Nature 375, 305–308.

Pflaumann, U., Jian, Zh., Pelejero, C., Heilig, S., Grimalt, J.O., 1999. Modern distribution patterns of planktonic foraminifera in the South China Sea and West Pacific: a new transfer technique to estimate regional sea-surface temperatures. Mar. Geol. 156, 41–83.

Prahl, F.G., Pinto, L.A., 1987. A geochemical study of long-chain n-aldehydes in Washington coastal sediments. Geochim. Cosmochim. Acta 51, 1573–1582.

Prahl, F.G., Wakeham, S.G., 1987. Calibration of unsaturation

patterns in long-chain ketone composition for paleotemperature assessment. Nature 330, 367–369.

Prahl, F.G., Muelhausen, L.A., Zahnie, D.A., 1988. Further evaluation of long-chain alkenones as indicators of paleoceanographic conditions. Geochim. Cosmochim. Acta 52, 2303–2310.

Prahl, F.G., Muelhausen, L.A., Lyle, M., 1989. An organic geochemical assessment of oceanographic conditions at MANOP site C over the past 26,000 years. Paleoceanography 4, 495510.

Sarnthein, M., Pflaumann, U., Wang, P.X., Wong, H.K. (Eds.), 1994. Preliminary report on Sonne-95 cruise 'Monitor Monsoon' to the South China Sea. Ber. Rep., Geol.-Paläontol. Inst. Univ. Kiel 68, 11–225.

Schönfeld, J., Kudrass, H., 1993. Hemipelagic sediment accumulation rates in the South China Sea related to Late Quaternary sea-level changes. Quat. Res. 40, 368–379.

Schubert, C.J., Stein, R., 1996. Deposition of organic carbon in Arctic Ocean sediments: terrigenous supply vs. marine productivity. Org. Geochem. 24, 421–436.

Sikes, E.L., Keigwin, L.D., 1994. Equatorial Atlantic sea surface temperature for the last 30 kyr: A comparison of $U_{37}^{K'}$, $\delta^{18}O$, and foraminiferal assemblage temperature estimates. Paleoceanography 9, 31–45.

Stuiver, M., Braziunas, T.F., 1993. Modeling atmospheric ^{14}C influences and ^{14}C ages of marine samples to 10,000 BC. Radiocarbon 35, 137–189.

Sun, X., Li, X., 1999. A pollen record of the last 37 ka in the deep sea core 17940 from the northern slope of the South China Sea. Mar. Geol. 156, 227–244.

Villanueva, J., 1996. Study of the oceanographic and climatic changes in the North Atlantic during the last 300,000 years by means of biomarker analysis. Ph.D. Dissertation, University Ramon Llull, Barcelona, Catalonia.

Villanueva, J., Pelejero, C., Grimalt, J., 1997. Clean-up procedures for the unbiased estimation of C_{37} alkenone sea surface temperatures and terrigenous *n*-alkane inputs in paleoceanography. J. Chromatogr. 757, 145–151.

Volkman, J.K., Eglinton, G., Corner, E.D.S., Sargent, J.R., 1980. Novel unsaturated straightchain C_{37}–C_{39} methyl and ethyl ketones in marine sediments and a coccolithophore *Emiliania huxleyi*. In: Douglas, A.G., Maxwell, J.R. (Eds.), Advances in Organic Geochemistry. Pergamon Press, Oxford, 1979 pp. 219–227.

Volkman, J.K., Barrett, S.M., Blackburn, S.I., Sikes, E.L., 1995. Alkenones in Gephyrocapsa oceanica: Implications for studies of paleoclimate. Geochim. Cosmochim. Acta. 59, 513–520.

Wang, L., Wang, P., 1992. Late Quaternary paleoceanography of the South China Sea: glacial–interglacial contrasts in an enclosed basin. Paleoceanography 5, 77–90.

Wang, L., Sarnthein, M., Erlenkeuser, H., Grimalt, J.O., Grootes, P., Heilig, S., Ivanova, E., Kienast, W., Pflaumann, U., Pelejero, C., 1999. East Asian monsoon climate during the Late Pleistocene: high-resolution sediment records from the South China Sea. Mar. Geol. 156, 245–284.

Wang, P., 1999. Response of Western Pacific marginal seas to glacial cycles: paleoceanographic and sedimentological features. Mar. Geol. 156, 5–39.

Winn, K., Sarnthein, M., Erlenkeuser, H., 1991. $\delta^{18}O$ stratigraphy and chronology of Kiel sediment cores from the East Atlantic. Berichte-Reports, Geol.-Palaeont. Inst. Univ. Kiel 45, 11–99.